^{1}H NMR ($CDCl_3$, 360 MHz) of this mixture showed a doublet (J = 2.1) at d 4.86 and a complex multiplet at d 4.44-4.57 ppm. The integrated areas of these peaks were in the ratio 5.76:1, corresponding to a 70:30 ratio of axial to equatorial attack. Capillary GC analysis (DB-17 column) revealed the presence of two products in the ratio 69:31. In the cases of substrates other than **7c** and **8c**, the ratio of equatorial to axial products was determined by ^{1}H NMR analysis of the reduction product mixture prior to acetylation. The ratios determined in this way were in good agreement with those determined by capillary GC analysis after acetylation.

Acknowledgment. We are grateful to the National Institutes of Health for financial support of this research, to Reza Goharderakhshan for technical assistance, and to Professor Michael N. Paddon-Row for helpful discussions and exchanges of unpublished results.

Molecular Dynamics of B-DNA Including Water and Counterions: A 140-ps Trajectory for d(CGCGAATTCGCG) Based on the GROMOS Force Field

S. Swaminathan,† G. Ravishanker, and D. L. Beveridge*

Contribution from the Chemistry Department, Hall-Atwater Laboratories, Wesleyan University, Middletown, Connecticut 06457. *Received November 13, 1990*

Abstract: A theoretical study of the dynamical structure of the DNA dodecamer d(CGCGAATTCGCG) based on 140 ps of molecular dynamics simulation including water and counterions is reported. The simulation involved the dodecamer and 1927 water molecules and 22 Na^+ counterions treated under periodic boundary conditions in a hexagonal prism elementary cell. The force field for the simulation is GROMOS supplemented with a restraint potential for maintaining Watson-Crick base pairing. Extensive Monte Carlo equilibration of the solvent was necessary to prepare the system in a suitable state to perform a stable dynamical trajectory. The structure at the termination of the trajectory resides clearly in the B-DNA family, 2.3 Å root-mean-square deviation from the corresponding canonical form. The analysis of the simulation reveals good accord with a number of features seen in the X-ray crystal structure of the dodecamer, including local axis deformation near the GC/AT interfaces in the sequence and large propeller twist in the base pairs. The narrowing of the minor groove in the AT region of the crystal structure is not observed over the time course of the simulation, but it may be a crystal-packing effect. The DNA base pairs show a consistent inclination in the simulation, in accord with the interpretation of results obtained from flow dichroism studies of DNA in solution. A comparison of the calculated dynamical structure with a recently proposed NMR structure of the dodecamer in solution is provided. In an additional simulation carried out without the Watson-Crick restraint function, more pronounced axis deformations and base pair openings are observed. A corresponding in vacuo simulation shows that explicit inclusion of the water molecules is necessary to properly support the major and minor groove structure of the DNA helix.

I. Introduction

Molecular dynamics (MD) simulation is a powerful theoretical and computational approach to the study of the structure and molecular motions of macromolecules,[1] and several free dynamics simulations have now been reported for DNA[2-11] and RNA[12] systems. The MD method together with a prescription for the molecular force field, a means of treating hydration and ion atmosphere effects, and a particular simulation protocol combine to produce a "dynamical model" of a DNA oligonucleotide on a picosecond level time scale. An accurate dynamical model for DNA can provide a general theoretical basis for understanding sequence-dependent fine structure and flexibility in DNA, and for subsequent studies of important drug-DNA and protein-DNA interactions. The issue currently at hand is the stability and accuracy of the various possible dynamical models of DNA obtained from MD simulation.

The treatment of environmental effects in the simulation differentiates dynamical models into two broad classes: in vacuo and solvated models. In vacuo models leave out explicit consideration of water and in some cases counterions as well. Some of the effect of water can be reintroduced by means of a distance-dependent dielectric screening of coulombic terms in the force field. counterions are included either explicitly[4] or implicitly by use of either reduced coulombic charges on the anionic phosphates of the DNA backbone[2,3] or a salt-dependent potential of mean force between phosphates.[13] The net dimensionality of the problem is thus considerably reduced in an in vacuo simulation model, and the calculations become feasible in a computer workstation environment. However, in the absence of water the model structure typically undergoes a contraction. Distortions affecting particularly residues on the surface, only a small fraction of a globular protein but nearly *all* of a DNA molecule, are also a possible problem.

The solvated models include water and counterions explicitly in the simulation, and thus provide a more realistic physical

† Present address: Pharmaceutical Research and Development Division, Bristol-Myers Squibb Company, 5 Research Parkway, Wallingford, CT 96492.

(1) McCammon; A. J.; Harvey, S. C. *Dynamics of Proteins and Nucleic Acids*; Cambridge University Press: Cambridge, 1986.
(2) Levitt, M. *Cold Spring Harbor Symp. Quant. Biol.* **1983**, *47*, 251.
(3) Tidor, B.; Irikura, K. K.; Brooks, B. R.; Karplus, M. *J. Biomol. Struct. Dyn.* **1983**, *1*, 231.
(4) Singh, U. C.; Weiner, S. J.; Kollman, P. A. *Proc. Natl. Acad. Sci. U.S.A.* **1985**, *82*, 755.
(5) Siebel, G. L.; Singh, U. C.; Kollman, P. A. *Proc. Natl. Acad. Sci. U.S.A.* **1985**, *82*, 6537.
(6) Van Gunsteren, W. F.; Berendsen, H. J.; Guersten, R. G.; Zwinderman, H. R. *Ann. N. Y. Acad. Sci.* **1986**, *482*, 287.
(7) Westhof, E.; Chevrier, B.; Gallion, S. L.; Weiner, P. K.; Levy, R. M. *J. Mol. Biol.*, **1986**, *190*, 699.
(8) Swamy, K.; Clementi, E. *Biopolymers* **1987**, *26*, 1901.
(9) Ravishanker, G.; Swaminathan, S.; Beveridge, D. L.; Lavery, R.; Sklenar, H. *J. Biomol. Struct. Dyn.* **1989**, *6*, 669.
(10) Srinivasan, J.; Withka, J. M.; Beveridge, D. L. *Biophys. J.* **1990**, *58*, 533.
(11) Zielinski, T. J.; Shibata, M. *Biopolymers* **1990**, *29*, 1027.
(12) Prabhakaran, M.; Harvey, S. C.; Mao, B.; McCammon, J. A. *J. Biomol. Struct. Dyn* **1983**, *1*, 357.
(13) Klement, R.; Soumpasis, D. M.; Kitzing, E. V.; Jovin, T. M. *Biopolymers* **1990**, *29*, 1089.

0002-7863/91/1513-5027$02.50/0

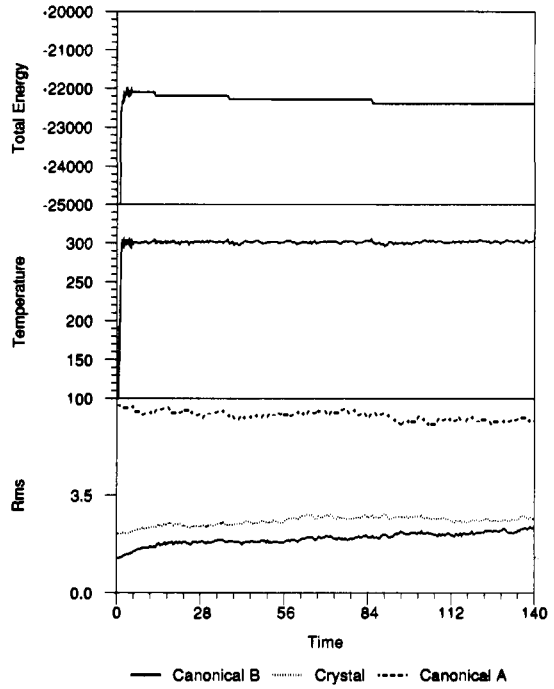

Figure 1. Calculated total energy, temperature, root-mean-square deviation from canonical A72 (dashed line) and B80 forms (solid line),[64,65] and the crystallographic native dodecamer (dotted line)[18] vs time for 140 ps of MD on duplex d(CGCGAATTCGCG) including water and counterions.

representation of the system. However, these simulations are of such high dimensionality that they are currently feasible only in a supercomputer environment or on a large-scale dedicated processor. Because of the sensitivity of DNA structure to environmental effects, including solvent explicitly is likely to be necessary for the development of an accurate dynamical model. This paper describes the behavior of the molecular dynamics of a solvated oligonucleotide dodecamer including counterions and water carried out on a CRAY YMP machine. A detailed comparison of the calculated results with related experimental data on the system is provided, and some general considerations on the methodological issues involved in the calculations are given. Overall, the results so far indicate that a reasonable dynamical model has been obtained.

The MD trajectories described herein for the dodecamer have been subsequently used by Withka et al.[14] to calculate theoretically quantities of interest in NMR spectroscopy, in particular the time evolution of the interproton NOE's. Such calculations will subsequently provide a basis for further evaluation of this and other dynamical models from NMR data on the solution structure of DNA oligonucleotides.

II. Background

The DNA system chosen for study is the dodecamer duplex of sequence d(CGCGAATTCGCG), important in molecular biology since the central GAATTC tract is the recognition site for the restriction enzyme Eco RI endonculease[15]. It is well-known from the early fiber diffraction studies of Franklin and Gosling[16] that right-handed DNA falls into two distinct families of structures, A and B. The A form is favored at lower humidity and the B form, similar to the double helix of Watson and Crick, is preferred at high humidity.[17] The d(CGCGAATTCGCG) structure was solved by Dickerson and co-workers[18] and found to be the first oligonucleotide to crystallize in the B form. Ten crystal structures of dodecamers of this sequence have now been reported.[18-30] Four of these involve bound drugs:[24,26,28,29] one structure is given in a preliminary report of a protein bound complex[27] and the others are free dodecamer under various conditions of temperature and derivatization.[18-23] There are several recent papers dealing with the NMR spectroscopy of this sequence,[31-33] and a solution structure has recently been proposed by Reid and co-workers.[34] Recently, the behavior of in vacuo models for d(CGCGAATTCGCG) based on the GROMOS,[35] AMBER[36] and CHARMM[37] force fields has been reported.

Experimental Studies. The structure of the free, uncomplexed form of d(CGCGAATTCGCG) serves as the main crystallographic point of reference for the theoretical calculations described herein. The first structure to be reported was based on data taken at 293 K[18,19] and is currently known as the native form, the "Dickerson dodecamer", or as recommended recently by Dickerson,[38] the HD dodecamer structure. The structure is quite clearly in the B form, with the base pairs disposed symmetrically with respect to the helix axis and oriented perpendicular to the axis in the AT region and only slightly tilted in the GC region. Beyond this, the crystal structure shows a number of deviations from the canonical B-DNA form, which inspired the proposition that the sequence-dependent fine structure may form an intrinsic code for the recognition of DNA by regulatory proteins.[39,40] Particularly notable is the propeller twist of the nucleotide pairs, larger in the AT then in the GC region (but neither negligible nor uniform in the latter), and inter-base pair hydrogen bonding in addition to the Watson–Crick base pairing at two places in the AATT region. There is a notable narrowing of the minor groove in the AATT region, which supports an ordered water network known as the "spine of hydration"[20] and a widening in the GC region consequent upon helix–helix crystal contacts. A sequence dependent in base pair roll is observed,[41] which follows quite well a theory on DNA bending set forth by Zhurkin.[42-44] Some degree of buckling and

(14) Withka, J.; Swaminathan, S.; Beveridge, D. L.; Bolton, P. H. *J. Am. Chem. Soc.* Following paper in this issue.
(15) Lewin, B. *Genes IV*; Oxford University Press: Oxford, 1990.
(16) Franklin, R. E.; Gosling, R. G. *Acta Crystallogr.* **1953**, *6*, 673.
(17) Saenger, W. *Principles of Nucleic Acid Structure*; Springer-Verlag: New York, 1983.
(18) Drew, H. R.; Wing, R. M.; Takano, T.; Broka, C.; Tanaka, S.; Itikura, K.; Dickerson, R. E. *Proc. Natl. Acad. Sci. U.S.A.* **1981**, *78*, 2179.
(19) Wing, R. M.; Drew, H. R.; Takano, T.; Broka, C.; Tanaka, S.; Itikura, I.; Dickerson, R. E. *Nature* **1980**, *278*, 755.
(20) Drew, H. R.; Dickerson, R. E. *J. Mol. Biol.* **1981**, *151*, 535.
(21) Drew, H. R.; Samson, S.; Dickerson, R. E. *Proc. Natl. Acad. Sci. U.S.A.* **1982**, *79*, 4040.
(22) Frantini, A. V.; Kopka, M. L.; Drew, H. R.; Dickerson; R. E. *J. Biol. Chem.* **1982**, *257*, 14686.
(23) Drew, H. R.; Samson, S.; Dickerson, R. E. *Proc. Natl. Acad. Sci. U.S.A.* **1982**, *79*, 4040.
(24) Wing, R. M.; Pjura, P.; Drew, H. R.; Dickerson, R. E. *EMBO J.* **1984**, *3*, 1201.
(25) Kopka, M. L.; Yoon, C.; Goodsell, D.; Pjura, P.; Dickerson, R. E. *Proc. Natl. Acad. Sci. U.S.A.* **1985**, *82*, 1376.
(26) Kopka, M. L.; Yoon, C.; Goodsell, D.; Pjura, P.; Dickerson, R. E. *J. Mol. Biol.* **1985**, *184*, 553.
(27) McClarin, J. A.; Frederick, C. A.; Wang, B. C.; Greene, P.; Boyer, H. W.; Grabel, J.; Rosenberg, J. M. *Science* **1986**, *234*, 1526.
(28) Pjura, P. E.; Grzeskowiak, K.; Dickerson, R. E. *J. Mol. Biol.* **1987**, *197*, 257.
(29) Teng, M.; Usman, U.; Frederick, C. A.; Wang, A. H. *Nucl. Acids Res.* **1988**, *16*, 2671.
(30) Larsen, T.; Goodsell, D.; Cascio, D.; Grzeskowiak, K.; Dickerson, R. E. *J. Biomol. Struct. Dyn.* **1989**, *7*, 477.
(31) Hare, D. R.; Wemmer, D. E.; Chou, S. H.; Drobny, G.; Reid, B. R. *J. Mol. Biol.* **1983**, *171*, 319.
(32) Patel, D.; Pardi, A.; Itakura, K. *Science* **1982**, *216*, 581.
(33) Ott, J.; Eckstein, F. *Biochemistry* **1985**, *24*, 2530.
(34) Nerdal, W.; Hare, D. R.; Reid, B. R. *Biochemistry* **1989**, *28*, 10008.
(35) van Gunsteren, W. F.; Berendsen, H. J. C. *GROMOS86: Groningen Molecular Simulation System*; University of Groningen, The Netherlands, 1986.
(36) Weiner, S. J.; Kollman, P. A.; Case, D. A.; Singh, U. C.; Ghio, C.; Alagona, G.; Profeta, S., Jr.; Weiner, P. *J. Am. Chem. Soc.* **1984**, *106*, 765.
(37) Nilsson, L.; Karplus, M. *J. Comp. Chem.* **1984**, *1*, 591.
(38) Dickerson, R. E. In *Structure; Methods.* Vol. 3. *DNA and RNA*; Sarma, R. H., Eds.; Adenine Press: New York, 1990; pp 1–37.
(39) Dickerson, R. E. *Sci. Am.* **1983**, *249*, 94.
(40) Dickerson, R. E.; Kopka, M. L.; Pjura, P. *Chem. Scr.* **1986**, *26b*, 139.
(41) Dickerson, R. E.; Drew, H. R. *J. Mol. Biol.* **1981**, *149*, 761.
(42) Zhurkin, V. B. *FEBS Lett.* **1983**, *158*, 293.
(43) Zhurkin, V. B. *J. Biomol. Struct. Dyn.* **1985**, *2*, 785.
(44) Sundaralingam, M.; Sekarudu, Y. C. In *Structure and Expression.* Vol. 3. *DNA Bending and Curvature*; Olson, W. K., Sarma, M. H., Sarma, R. H., Sundaralingam, M., Eds.; Adenine Press: New York, 1988; pp 9–23.

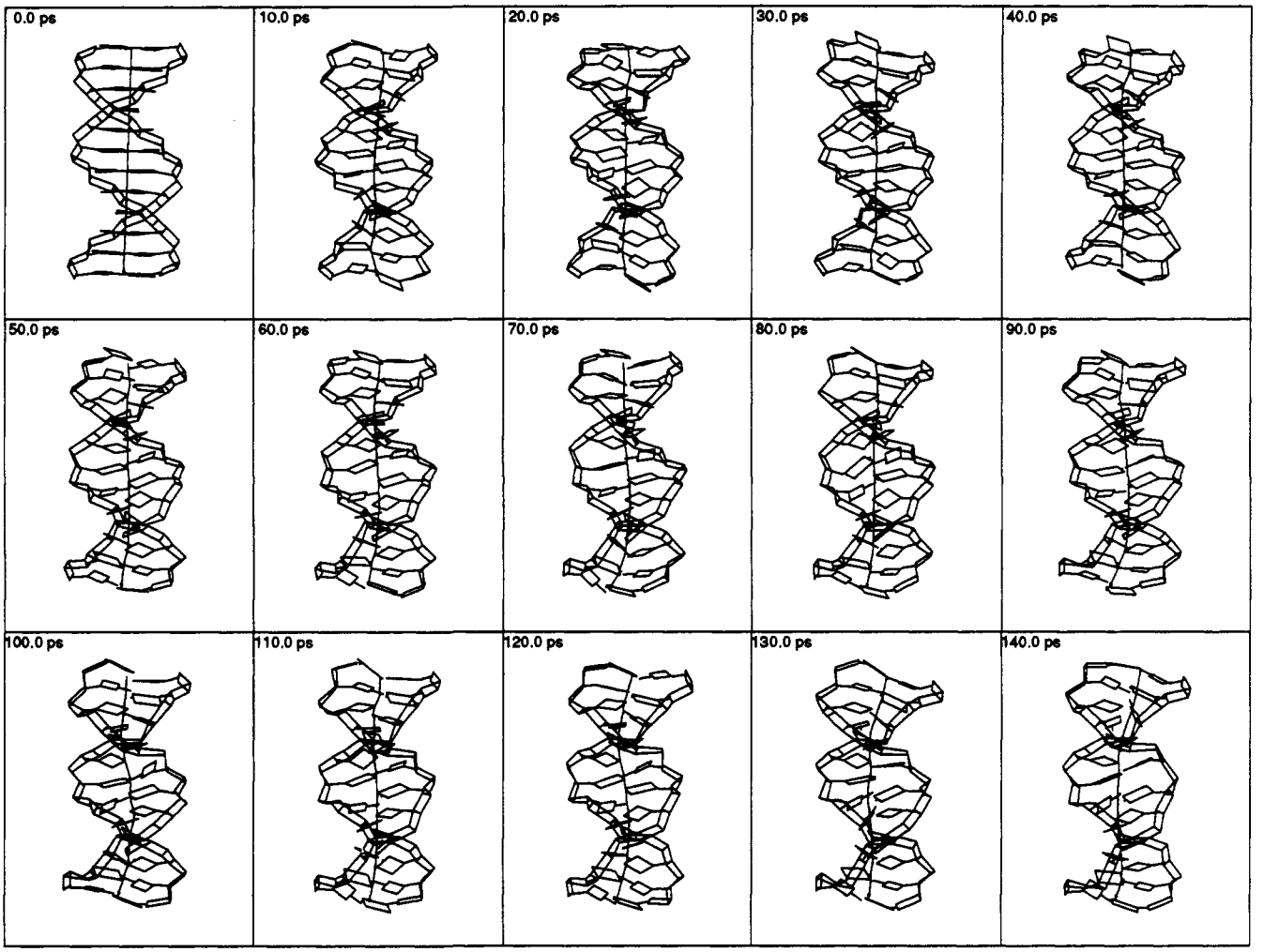

Figure 2. A sequence of snapshots of the structure of d(CGCGAATTCGCG) at evenly spaced intervals along the 140-ps MD trajectory. The structure in the upper left hand panel is the canonical B80[65] form used as a starting configuration.

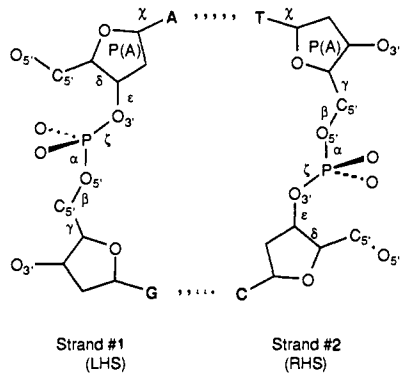

Figure 3. A base pair step and designation of IUPAC conformational parameters[77] used in conformational Dials analysis for nucleic acids.

base pair opening is seen in the crystal structure, the latter particularly in the AT region. The helix axis is observed to exhibit a local deformation at steps C3pG4 and to a lesser extent at C9pG10, termed the "roll points" by Dickerson and co-workers.[22]

Independent structure determinations at 16 K[23] and of 5-bromocytosine derivatives at 20 K (MD20) and 7 K (MPD7)[22] have been reported, and show considerable fine structure homology with the native dodecamer. The helix axis of the MDP7 structure is somewhat straighter than the others, particularly at the upper roll point, indicating that the observed axis irregularities may be intrinsic to the DNA and not a crystal packing effect. Anisotropic refinement on the dodecamer was reported by Holbrook et al.[45] and provides additional detail on local atomic and group mobilities.[46]

Examination of the structure of the drug- and protein-bound dodecamers[27,47] in comparison with the uncomplexed forms reveals some small differences, but are more remarkable in their similarities. Axis deformations at or near the roll points persist in all structures. The localized ("annealed") bends are quite pronounced in the dodecamer–Eco RI endonuclease complex, where they have been termed "neo-kinks".[27]

NMR studies of d(CGCGAATTCGCG) in solution led to the assignment of all proton resonances.[31,32] NMR studies generally indicate that Watson–Crick base pairing is well-maintained in solution with hydrogen exchange occurring only infrequently with respect to the MD time scale.[48] Ott and Eckstein[33] assigned the individual ^{31}P NMR resonances of the dodecamer. Anomalous chemical shifts at steps 3 and 9 were observed and interpreted as an indication of a break in conformation at these locations, which correspond to the roll points in the crystal structure.

The use of MD simulation with 2D-NOESY restraints from NMR has been used in recent structural predictions for several DNA oligonucleotides.[49-53] Recently, Nerdal, Hare, and Reid[54]

(45) Holbrook, S. R.; Dickerson, R. E.; Kim, S. H. *Acta. Cryst. Sect. B, Struct. Sci.* **1985**, *b41*, 255–262.
(46) Holbrook, S. R.; Kim, S.-*J. Mol. Biol.* **1984**, *173*, 361.
(47) Goodsell, D.; Dickerson, R. E. *J. Med. Chem.* **1986**, *29*, 727.
(48) Moe, J. G.; Russu, I. M. *Nucleic Acids Res.* **1990**, *18*, 821.
(49) Nilsson, L.; Clore, G. M.; Gronenborn, A. M.; Brunger, A. J.; Karplus, M.*J. Mol. Biol.* **1986**, *188*, 455.
(50) Nilges, M.; Clore, G. M.; Gronenborn, A.; Piel, N.; McLaughlin, L. W. *Biochemistry* **1987**, *26*, 3734.
(51) Nilges, M.; Clore, G. M.; Gronenborn, A.; Brunger, A. T.; Karplus, M.; Nilsson, L. *Biochemistry* **1987**, *26*, 3718.
(52) Behling, R. W.; Rao, S. N.; Kollman, P. A.; Kearns, D. R. *Biochemistry* **1987**, *26*, 4674.

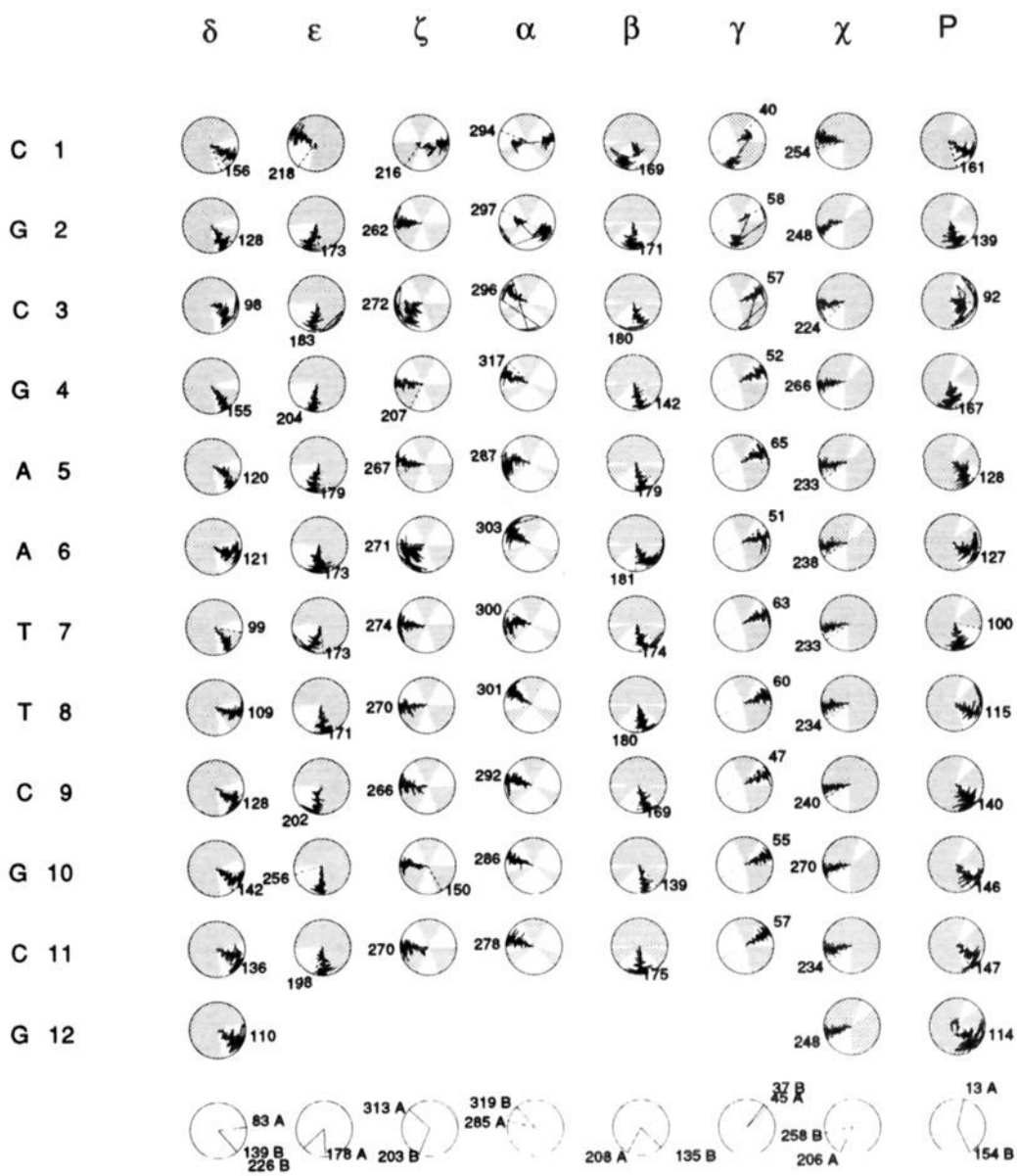

Figure 4. Conformational dials for the analysis of the dynamical behavior of strand 1 of d(CGCGAATTCGCG). The radical coordinate is the time axis, with $t = 0$ ps at the center and $t = 140$ ps at the circumference. The values assumed in the native HD dodecamer crystal structure[18] are indicated by solid lines. The shading indicates the sterically forbidden regions of conformational space as delineated by Olson.[63]

have proposed a solution structure for d(CGCGAATTCGCG) at room temperature based on refinement of NMR derived distance geometry structure and NOESY spectrum back-calculations on 155 interproton distances. The proposed solution structure appears to be somewhat different from those observed in the crystal. The position of the NMR resonances indicates perfect palindromic symmetry for the dodecamer in solution. The structures are not symmetric, even though the base pair sequence is self-complimentary, in the lower symmetry environment of the crystal. Evidence for kinks in the structure of the C3pG4 (and the symmetry equivalent position C9pG10) and A6pT7 junctions is described. The former involves an opening into the minor groove caused by base pair roll, and the latter involves slide and some opening into the major groove. The minor groove is narrowed in the AT region and broadened in the peripheral GC tracts.

Nerdal et al. analyzed the structure and found it to be highly underwound with respect to either canonical A and B forms of DNA, and markedly so at steps C3pG4 and C9pG10. This anomaly was linked to an atypical sugar conformation at G4 and G10, a consequence of a abnormally short NOE distance between H_8 of A5 and $H_{1'}$ of G4. The kink at the A6pT7 step is linked to a high propeller twist and a reasonably large roll value combined with negative helical slide. The crystal structures of the dodecamer display corresponding roll points but to a lesser degree than that inferred from the NMR analysis. The axis deformations in the NMR and crystal structures lead to an indication of overall bending for the duplex Eco RI sequence, which is supported by data for polyacrylamide gel electrophoresis on related decamer sequences by Diekmann and McLaughlin.[55]

Theoretical and Computational Studies. Levitt[2] first reported 90 ps of molecular dynamics on the duplex d(CGCGAATTCGCG) and a dA·dT 24-mer with a vacuum boundary, omitting electrostatic terms in the nonbonded interactions. The simulation demonstrated an overall stability, but also large-amplitude bending and twisting, affecting the major groove anisotropically. Time-lapse structures were presented and

(53) Metzler, W. J.; Wang, C.; Kitchen, D. B.; Levy, R. M.; Pardi, A. *J. Mol. Biol.* **1990**, *214*, 711.
(54) Nerdal, W.; Hare, D. R.; Reid, B. R. *Biochemistry* **1989**, *28*, 10008.
(55) Diekmann, S.; McLaughlin, L. *J. Mol. Biol.* **1988**, *202*, 823.

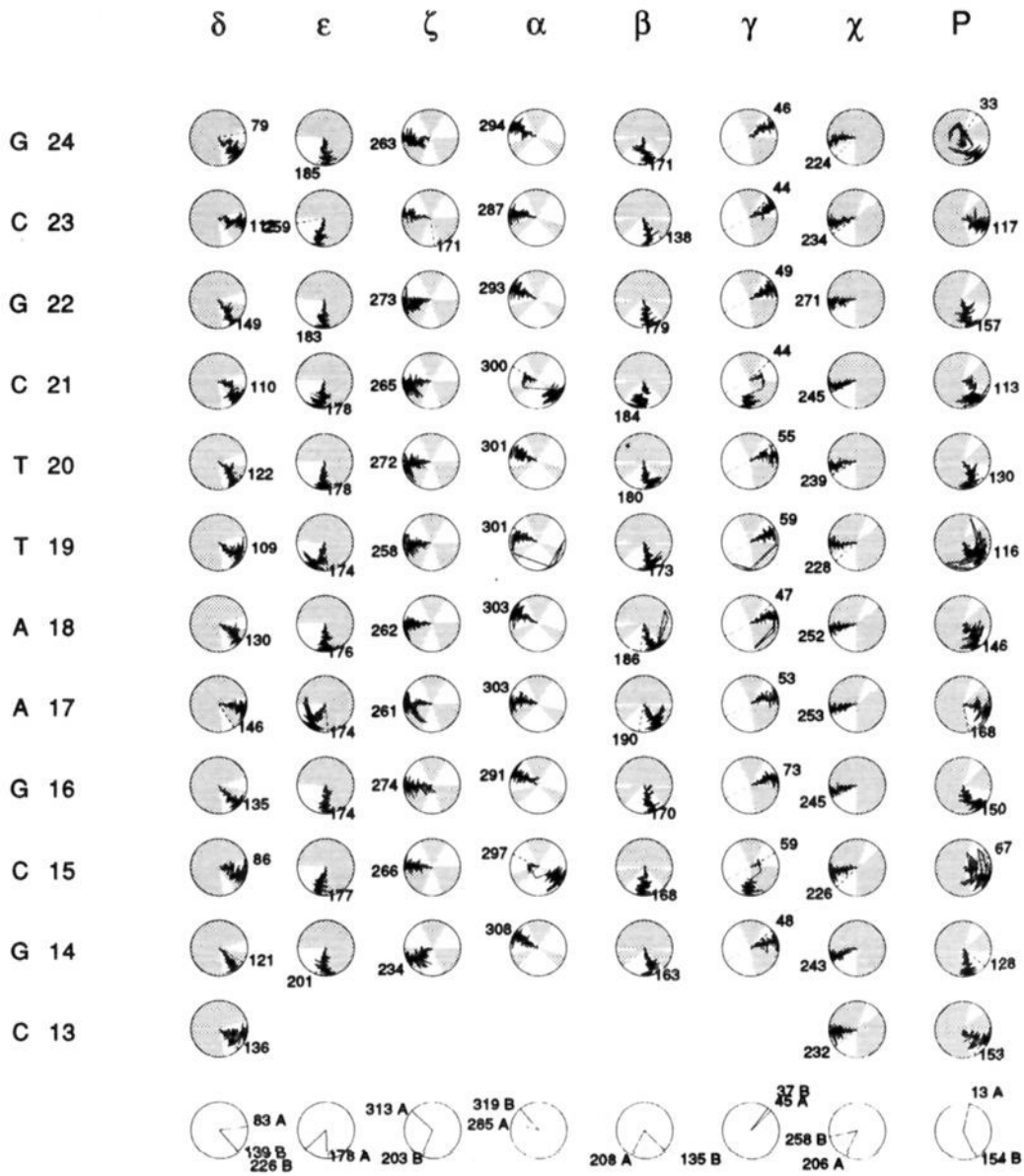

Figure 5. Conformational dials for the analysis of the dynamical behavior of strand 2 of d(CGCGAATTCGCG). The radical coordinate is the time axis, with $t = 0$ ps at the center and $t = 140$ ps at the circumference. The values assumed in the native HD dodecamer crystal structure[18] are indicated by solid lines. The shading indicates the sterically forbidden regions of conformational space as delineated by Olson.[63]

considerable informative details of the motions and were analyzed and reported. Some estimates of electrostatic effects were made, but when charges were added to the model at an internal dielectric of unity the duplex unwound. Subsequently, there have been several proposals for MD force fields with capabilities for treating nucleic acids, including AMBER,[36] GROMOS[35] and CHARMM[37]. Each of these has been used in specific studies of DNA with some degree of success, but little in the way of comparative studies has yet been reported.

We have been undertaking a series of computational studies aimed at comparing the performance of the various force fields proposed for DNA in MD simulation and characterizing the behavior of MD of DNA based on in vacuo and solvated models. To facilitate this, a format for the comprehensive analysis of duplex DNA structure and dynamics has been developed. The essential procedure for the analysis is based on the "Curves" algorithm developed by Lavery and Sklenar.[56] The presentation of results is based on the computer graphics display called "Dials and Windows" proposed by Ravishanker et al.,[9] and illustrated with an in vacuo study of d(CGCGAATTCGCG) based no the GROMOS force field. This analysis procedure, subsequently referred to as "Curves, Dial and Windows" (CDW) is used extensively in the study described herein.

The behavior of an in vacuo model of d(CGCGAATTCGCG) in molecular dynamics simulation based in the AMBER force field has recently been described by Rao and Köllman[57] and by Srinivasan et al.[10] treating the DNA together with Na^+ ion with expanded radii representative of a "hydrated" counterion. We found that over the course of ca. 100 ps of MD simulation that the base pairs are nearly symmetric with respect to the helix axis as in B-DNA but have a net inclination similar to that of the A form. High-amplitude buckling and propeller twist are seen in the base pairs, with significant though oscillatory axis bending in the vicinity of the crystallographic roll points. Trajectories initiated at either canonical B-DNA or canonical A-DNA transit to the same intermediate structural form, and thus A- and B-DNA do not seem to be well-differentiated by in vacuo AMBER.

Louise-May et al. have carried out a study of in vacuo models

(56) Lavery, R.; Sklenar, H. *J. Biomol. Str. Dyn.* **1988**, *6*, 63.

(57) Rao, S. N.; Köllman, P. A. *Biopolymers* **1990**, *29*, 517.

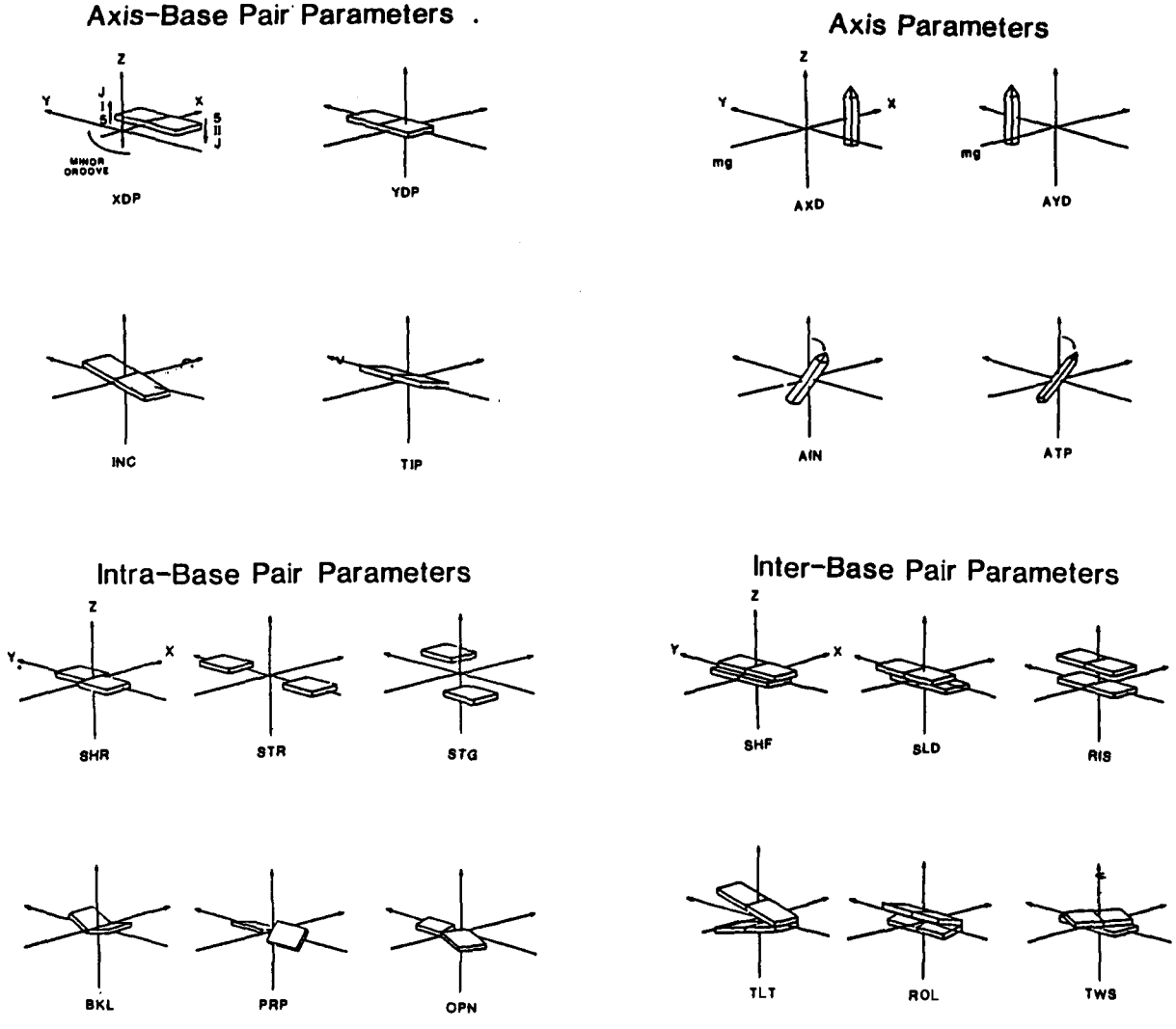

Figure 6. Helicoidal parameters of nucleic acids used in "Curves" analysis.[67]

of A and B d(CGCGAATTCGCG) in MD simulation based on the CHARMM force field.[58] This force field supports well-differentiated forms of A- and B-DNA, with oscillatory behavior exhibiting a generally narrower range of motion than in AMBER. Further studies and a detailed comparison of the results of in vacuo simulations on A- and B-DNA with use of the GROMOS, AMBER, and CHARMM force fields will be forthcoming.[59] However, it appears at this point that including solvent effects correctly will be essential to accurately describe the DNA dynamics in solution, with hydration, ion solvation, and electrostatic shielding effects in a proper balance with the intramolecular forces.

III. Calculations

The simulations reported herein involve energy minimization, Monte Carlo calculations, and molecular dynamics simulation with use of the programs GROMOS[35] and WESDYN[60] implemented on the CRAY YMP supercomputer at the Pittsburgh Supercomputer Center. The force field and molecular topology were obtained from PROGMT of GROMOS. We configure the system as the dodecamer duplex d-(CGCGAATTCGCG) together with 22 Na^+ counterions and explicit water in a hexagonal prism cell treated in the simulation under periodic boundary conditions. A total of 1927 water molecules was included, enough to provide in excess of two complete hydration shells for the DNA at an environmental density of ~ 1 g/cm^3.

The GROMOS force field with the addition of a harmonic constraint function (k_H = 5 kcal/mol) for hydrogen bonds involved in Watson–Crick base pairing was used for the DNA. The simple point charge (SPC) model,[61] which reproduces the radial distribution and dielectric behavior of pure water reasonably well, was used for the solvent. Switching functions were used to make the nonbonded interactions of all types go smoothly to zero between 7.5 and 8.5 Å, consistent with the parametrization of SPC water. To avoid artificially splitting dipoles, the nonbonded pair list was formed on a group-by-group basis where the groups correspond to sets of atoms comprising well-defined chemical subunits that on the basis of structural chemistry can be assumed to be electrically neutral. The Na^+ are grouped with phosphates in these procedures, which assures that all mobile counterions will always be included in the pair interaction list.

An initial configuration for the NaDNA complex was generated with the Na^+ positioned 6 Å from the phosphorus atom along the OPO bisector. A Monte Carlo Metropolis sampling of 10K passes was applied to the Na^+ in the absence of water, with the DNA structure fixed in the canonical B80 form. A restraint potential with a minimum at 4.5 Å and a force constant of 25 (kcal mol^{-1})/Å^2 was used to tether the sodium ions during this step, aimed at simply positioning the Na^+ in a reasonable geometry with respect to the DNA. The water molecules were then added to the NaDNA on a grid, and the water subjected to 10000 passes of MC equilibration.

The Na^+ restraint was next adjusted to a hemiharmonic form, which kept the sodium ions within 6 Å of the PO_2^- but otherwise allowed them to move in the simulation. Another 10K passes of MC equilibration were applied to the water and Na ions together. Finally, all restraints were removed and 5K passes of free MC equilibration were carried out on the water and counterions. The average total energy and the component

(58) Louise-May, S.; Beveridge, D. L. Submitted for publication.
(59) J. Srinivasan and D. L. Beveridge, manuscript in preparation.
(60) Swaminathan, S. *WESDYN*; Wesleyan University: Middletown, CT, 1990.
(61) Berendsen, H. J. C.; Postma, J. P. M.; van Gunsteren, W. F.; Hermans, J. In *Intermolecular Forces*, Pullman, B., Ed.; D. Reidel: Dordrecht, 1981; pp 331–342.

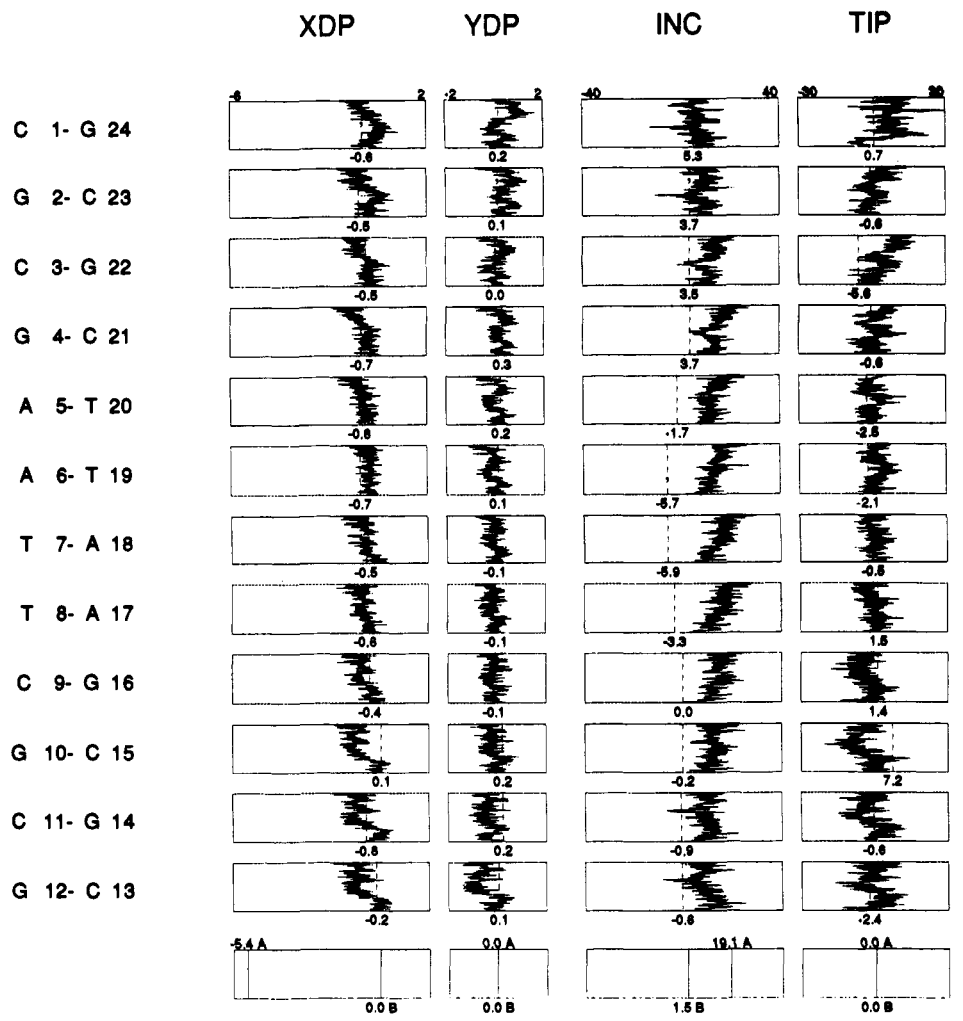

Figure 7. Helicoidal windows for the analysis of the dynamical behavior of axis-base pair parameters for d(CGCGAATTCGCG). The values assumed in the native HD dodecamer crystal structure[18] are indicated by dashed lines. The vertical direction is the time axis, with t = 0 ps at the bottom and t = 140 ps at the top.

solute–solvent and solute–solute and solvent–solvent were observed to be quite stable, and the solvent was considered to be well-equilibrated in the field of the DNA.

Next, 50 steps of conjugate gradient minimization were applied to the entire system, to relieve any residual clashes of atoms within the DNA. This was followed by 1.5 ps of heating of the system to ca. 300 K, 3.5 ps of Gaussian equilibration at 300 K, and 35 ps of free equilbration at 300 ± 4 K. A subsequent MD trajectory of 100 ps was then carried out. The MD steps required a total of 40 h on the CRAY YMP. The convergence profiles of total energy and temperature for the MD simulation steps are shown in Figure 1. The stability of the calculation is quite notable, indicative of a well-behaved simulation and a stable dynamical structure for the DNA.

The above procedure was adopted after a considerable number of exploratory calculations, a brief description of which may be of interest to practioners. Initially, we tried a protocol in which the counterions were initially placed at the bisector of the OPO bond angle at a distance of 3.5 Å from each phosphate. The water molecules were added at random orientations on a uniform grid of the simulation cell. Initially, an unrestrained MD equilibration was attempted. Extensive counterion diffusion occurred, first away from the DNA to ca. 6–8 Å and then back toward it. This process was very slow and time consuming, and a satisfactory equilibration was not achieved even after 40 ps of MD trajectory. We also observed considerable instability in the DNA conformational structure. This led us to the revised procedure described above. The heating step for the other protocols that were tried led initially to a large hump in the total energy curve, indicative of a metastable solvent structure which was slow to dissipate. the MD heating step after the current extensive MC equilibration procedure lands the system directly at a total energy (and presumably structure) close to the final equilibrated value, from which the MD was found to proceed in a reasonable manner.

Two additional simulations are provided as reference points. One was similar in all respects to that described above, except that the restraint on the Watson–Crick base pairing was removed leaving only the coulombic effects of the net atomic charges to hold the base pairs together. The other[59] was an in vacuo simulation using reduced charge on the phosphate of magnitude −0.25 and including "solvatons" of charge +0.25 as counterions for electroneutrality. The former provides perspective on the effect of the restraints, and the latter on the effect of neglecting explicit consideration of water in the simulation.

IV. Results

A sequence of structures which represent the calculated dynamical trajectory for d(CGCGAATTCGCG) is shown in Figure 2. The double helix remains obviously intact over the course of the simulation. However, considerable irregularities develop in the dynamical structure as compared with canonical B. We proceeded using CDW analysis to investigate the nature of the calculated dynamical structure, with regard to both general questions such as the extent to which the dodecamer model maintains a B-form structure over the course of the simulation and specific details such as the conformational transitions, sugar repuckerings, and the nature of helicoidal variations observed in the trajectory.

The conformational coordinates as used in the CDW analysis are defined in Figure 3. The conformational dynamics of this dodecamer are shown in Figures 4 and 5 for the two strands of the duplex, respectively. The conventions adopted in this analysis are fully described in a previous article by Ravishanker et al.[9] Briefly, each of the 206 backbone angles α, β, γ, δ, ϵ, ζ and the exocyclic angle χ is analyzed with use of a Klyne–Prelog[62] conformational dial. The sugar puckers P are analyzed with pseudorotation dials.[17] The layout of the dial system in the computer graphics is isomorphic with the structure per se, 5′ to 3′ on one

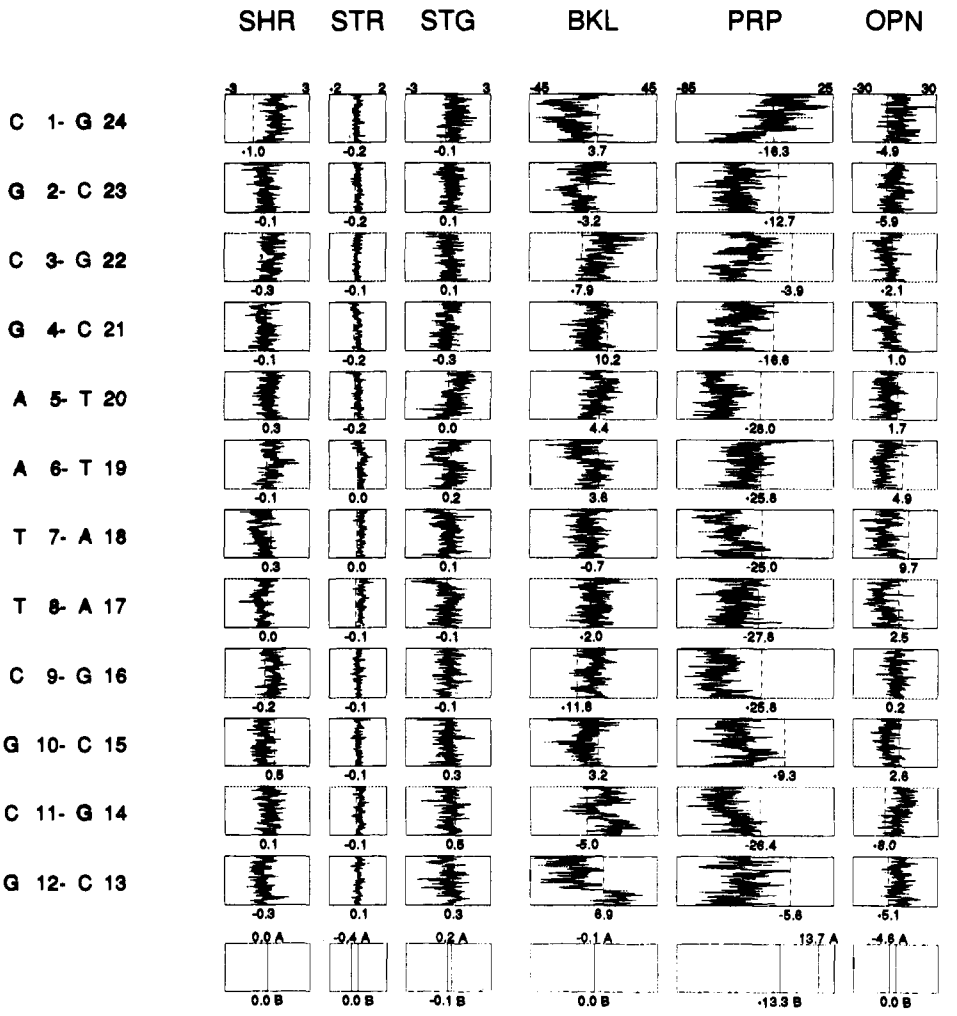

Figure 8. Helicoidal windows for the analysis of the dynamical behavior of intra-base pair parameters for d(CGCGAATTCGCG). The values assumed in the native HD dodecamer crystal structure[18] are indicated by dashed lines. The vertical direction is the time axis, with t = 0 ps at the bottom and t = 140 ps at the top.

strand, arbitrarily designated "left hand", and 3′ to 5′ on the "right-hand" strand. The order of the dials is based on a sequence which places the phosphodiester torsion angles (α and ζ) centrally within the dial system for a given nucleotide step. The phosphodiester torsions for base pair steps on opposite strands thus appear in corresponding interior positions for the left- and right-hand set of dials. The radius of the conformational dials is taken as the 140-ps time coordinate of the dynamics, with the origin t = 0 at the center. Each dial thus contains a complete record of the dynamical trajectory of the corresponding structural parameter in the course of the simulation. The dashed line in each dial specifies the value of the corresponding parameter in the native HD dodecamer crystal structure. Shaded areas indicate the sterically forbidden regions for each conformational parameter predicted by Olson[63] and for the sugar puckers by Dickerson.[38] Dials for the canonical A72[64] and B80[65] structural forms are given at the bottom of Figures 4 and 5 for reference.

The Dials analysis of the MD trajectory for the dodecamer reveals the parameter δ in the interior of the furanose sugar ring to be relatively stable over the time course of the simulation and oscillating freely in the sterically permitted region in the vicinity of (+)-anticlinal to (+)-antiperiplanar. The backbone parameter ϵ is generally stable in the antiperiplanar region with the exception of a transition t to g^- at C1, probably an end effect, and a transition $t \rightarrow (g^-) \rightarrow t$ at A17, where the parentheses indicate a transitory form. This is correlated with a multiple transition $g^- \rightarrow (t) \rightarrow g^-$ in the phosphodiester torsion ζ at A17, which is otherwise reasonably stable in the region of a high g^-. The behavior observed in the simulation at A17 is essentially a transient B_I to B_{II} transition.[66]

The phosphodiester torsions α and γ show the most dynamical activity in the trajectory, with conformational transitions observed in 6 out of 24 cases. The transitions in α and γ are highly correlated. The parameter β intervening between α and γ is conformationally stable, and oscillates with a narrow dynamical range in the antiperiplanar region, i.e. trans. The correlated transitions in α and γ, separated by β, define a "crankshaft motion" of the conformational dynamics, in which compensatory changes in two individual torsion angles take place in such a way that the helix is conserved.

For the sugar puckers, clearly the C_2'-endo structure typical of a B form of DNA gives way to C_1'-exo in the simulation. In a few cases, there is transient repuckering to the C_3'-endo value characteristic of an A-DNA. The sugar puckering remains dynamically active even at the termination of the trajectory.

The definition of the helicoidal parameters involved in the analysis is given in Figure 6. Analysis of the dynamical evolution of the helicoidal parameters for the dodecamer is shown in Figures 7–10. A set of 20 helicoidal parameters are involved and are divided into four groups; axis-base pair (4), intra-base pair (6),

(62) Klyne, W.; Prelog, V. *Experimentia* **1960**, *16*, 521.
(63) Olson, W. In *Topics in Nucleic Acid Structure*; Neidle, S., Eds.; MacMillan, Ltd.: London, 1982; Part 2, pp 1–76.
(64) Arnott, S.; Hukins, D. W. L. *Biochem. Biophys. Res. Commun.* **1972**, *47*, 1504.
(65) Arnott, S.; Chandrasekeharan, R.; Birdsall, D. L.; Leslie, A. G. W.; Ratliffe, R. L. *Nature* **1980**, *283*, 743.
(66) Gupta, G.; Bansal, M.; Sasisekharan, V. *Proc. Natl. Acad. Sci. U.S.A.* **1980**, *77*, 6486.

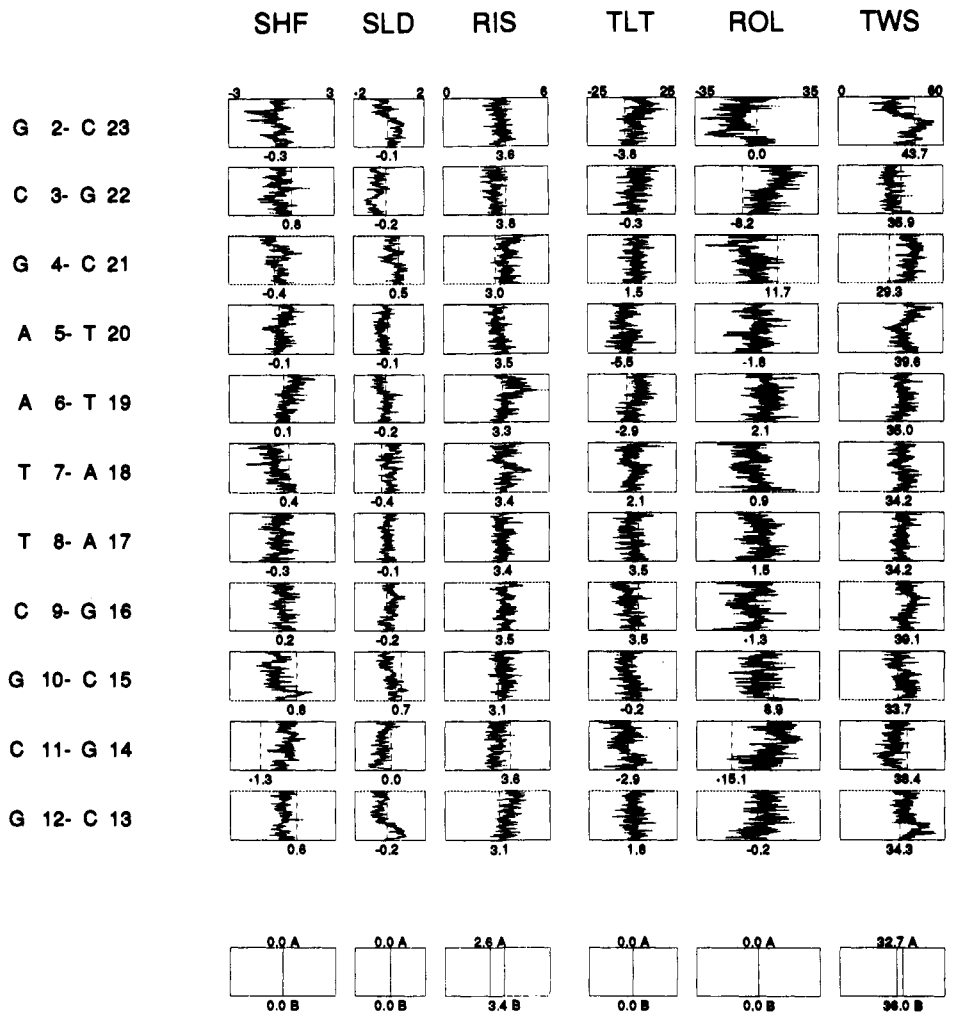

Figure 9. Helicoidal windows for the analysis of the dynamical behavior of inter-base pair parameters for d(CGCGAATTCGCG). The values assumed in the native HD dodecamer crystal structure[18] are indicated by dashed lines. The vertical direction is the time axis, with $t = 0$ ps at the bottom and $t = 140$ ps at the top.

inter-base pair (6), and axis-junction parameters (4). The helical axis is obtained in a Curves analysis by minimizing a function that describes simultaneously the change in orientation between successive nucleotides and the nonlinearity of the helicoidal axis. The optimal helicoidal solution produces the overall helical axis that best fits the conformation considered, with structural irregularity distributed between changes in the axis-base pair parameters and axis curvature. The results on helicoidal parameters pertaining to successive nucleotide base pairs are laid out in the graphics as "windows", defined on a suitable range of values for each parameter. The time axis is on the vertical, increasing from bottom to top in these figures. The dotted lines in each of the windows represent the corresponding crystal values for the native dodecamer. As with the dials, the layout of the windows represents the structure as viewed with the 5′–3′ polarity of the left-hand strand running down the page. Full details on the helicoidal parameters are given elsewhere.[9,56,67]

The results for the axis base-pair parameters X-displacement (XDP), Y-displacement (YDP), inclination (INC), and tip (TIP) are shown in Figure 7. The parameter XDP is critical in differentiating the canonical B form of DNA (−0.71 Å) from the A form (−5.43 Å). On the basis of XDP, the dodecamer definitely remains in the B range over the entire MD trajectory. The dynamical behavior of XDP is that of rapid oscillatory motion of the picosecond time scale with an apparent slower motion (grand cycle) superimposed toward the ends of the helix. The alternative possibility of an incipient instability in the helix cannot be ruled out without extending the trajectory, but we consider it unlikely in light of the WC restraints and the number of other cases in which we have definitively observed grand cycle behavior in DNA simulations.[58,59] The parameter YDP is stable. The parameters INC and TIP specify the orientation of the base pairs with respect to the helical axis. The INC parameter transits to an intermediate form between canonical B and A forms of DNA, particularly in the AT region. The parameter TIP is dynamically stable.

The dynamical behavior of the intra-base parameters is shown in Figure 8. The distance parameters shear (SHR), stretch (STR), and stagger (STG) are all relatively stable. A large propeller twist in the base pairs (negative in the new convention[68]) is assumed quite spontaneously in the dynamical model, and stabilizes at values of ~30°. The value of PRP at C1G24 goes back to near zero, but this may be an end effect. The parameter OPN is marginally larger for AT compared with GC base pairs, a consequence of two hydrogen bonds in the former vs three in the latter. This is not, however, a pronounced effect.

The dynamical behavior of the interbase pair parameters is shown in Figure 9. Shift (SHF), slide (SLD), and rise (RIS) parameters are oscillatory and stable. The parameter ROL shows evidence of a positive displacement at or near the axis deformations, indicating an opening toward the minor groove. The base

(67) Lavery, R.; Sklenar, H. *J. Biomol. Struct. Dyn.* **1989**, *6*, 655.

(68) Dickerson, R. E.; Bansil, M.; Calladine, C. R.; Diekmann, S.; Hunter, W. N.; Kennard, O.; von Kitzing, E.; Lavery, R.; Nelson, H. C. M.; Olson, W. K.; Saenger, W.; Shakked, Z.; Sklenar, H.; Soumpasis, D. M.; Tung, C. S.; Wang, A. H. J.; Zhurkin, V. B. *EMBO J.* **1989**, *8*, 1.

(69) Dougherty, A. M.; Causley, G. C.; Johnson, W. C., Jr. *Proc. Natl. Acad. Sci. U.S.A.* **1983**, *80*, 2193.

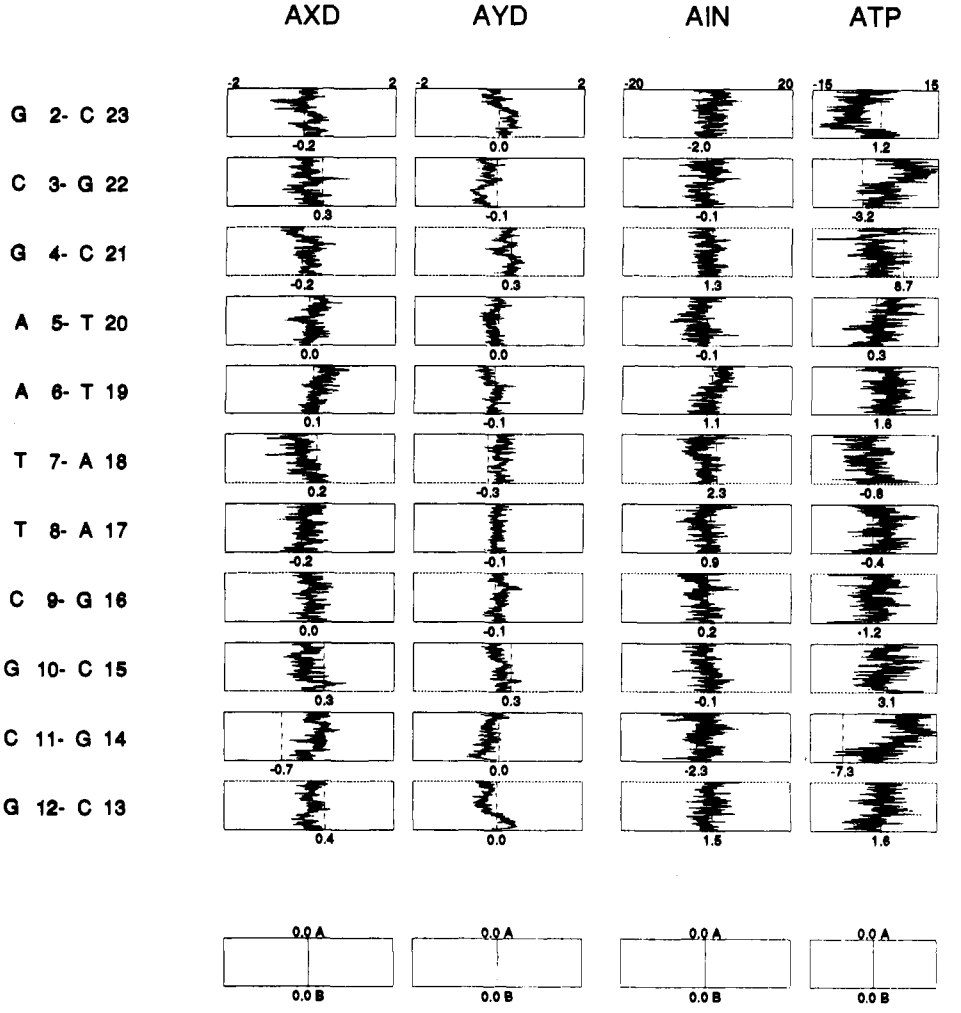

Figure 10. Helicoidal windows for the analysis of the dynamical behavior of axis-junction pair parameters for d(CGCGAATTCGCG). The values assumed in the native HD dodecamer crystal structure[18] are indicated by dashed lines. The vertical direction is the time axis, with t = 0 ps at the bottom and t = 140 ps at the top.

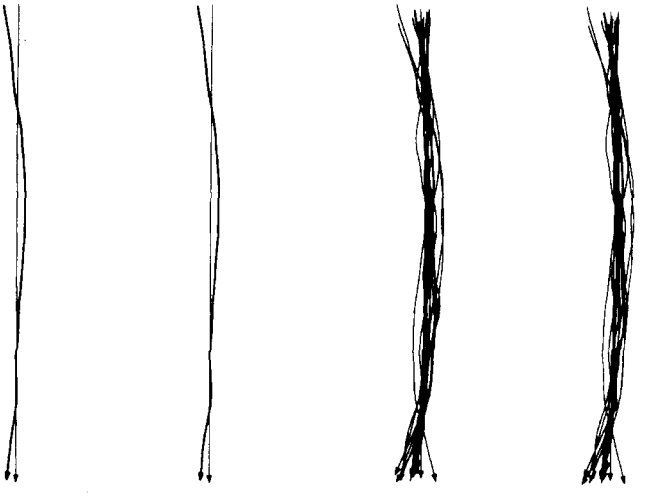

Figure 11. Calculated helix axes for various d(CGCGAATTCGCG) dodecamers: (a) the helix axis of canonical B-DNA (straight dark line) and the HD dodecamer (other dark line); (b) superposition of helix axes from the MD snapshots, indicating the dynamical range of axis motion.

pair RIS value in the dynamical structure remains in all cases at or near the value for canonical B-DNA. The values of TWS remain essentially in the realm of canonical B values, although an incipient underwinding can be discerned at or near the roll points.

The axis parameters (Figure 10) are generally oscillatory, with obvious displacements in ATP occurring at the C3 and C11 steps.

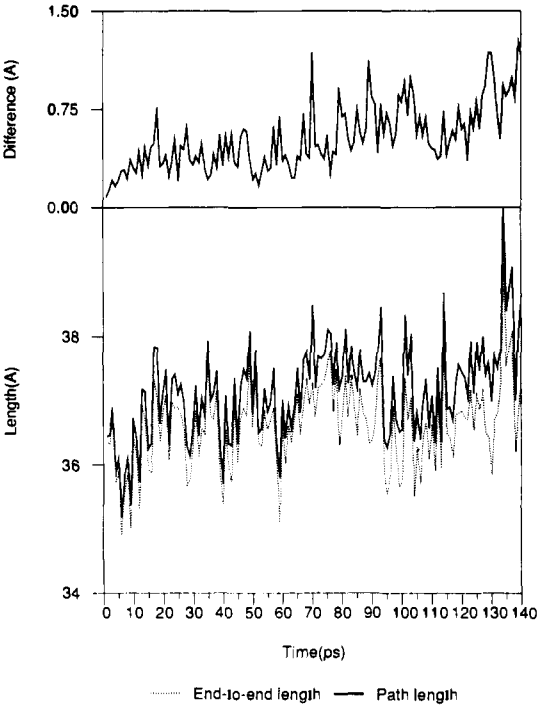

Figure 12. Calculated path length of the helix axis, end-to-end distance, and the difference of these two functions plotted against time for the 140-ps dynamical trajectory.

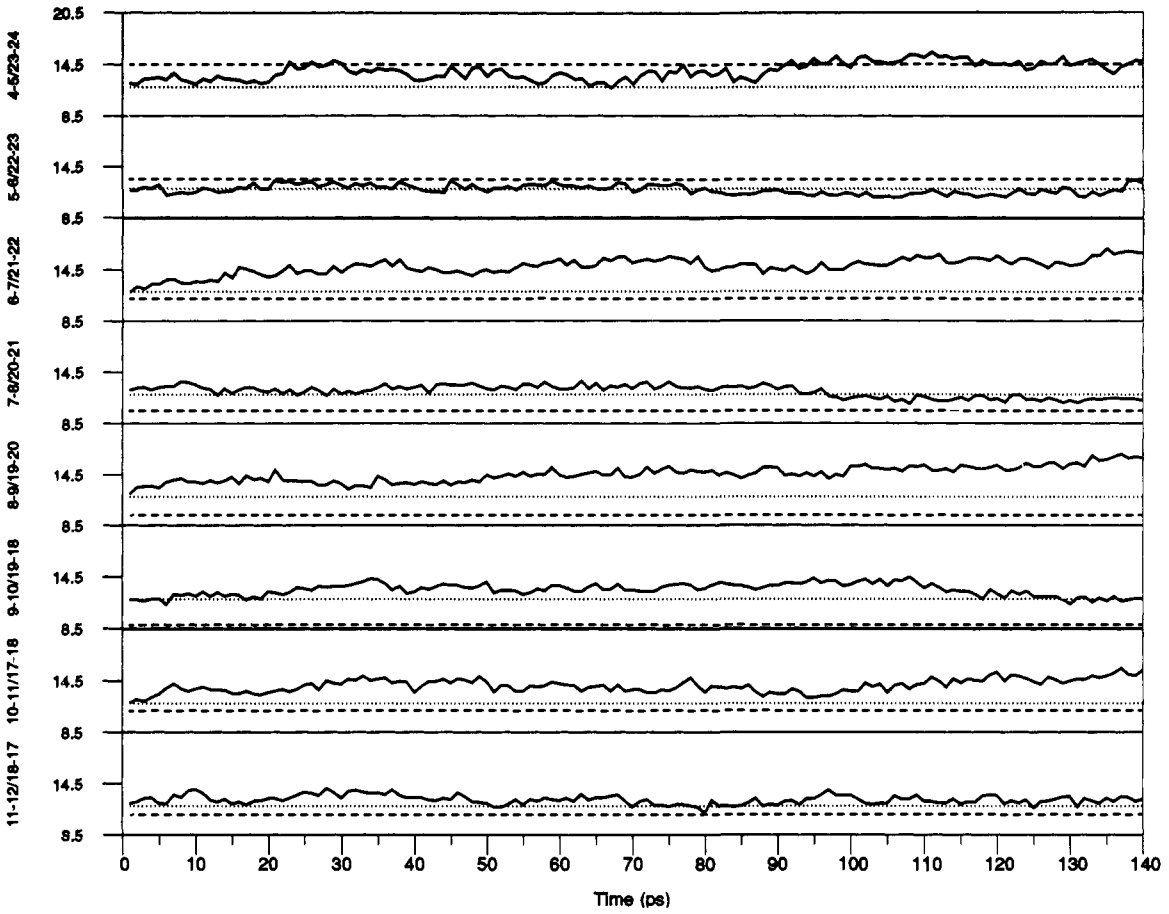

Figure 13. Calculated dynamical behavior of the major groove inter-phosphate distances (Å) for the dodecamer at various points in the sequence as a function of time: (---) canonical B80 values; (···) native dodecamer.

V. Discussion and Further Analysis

The dynamical model described above, as evidenced by the appearance of the snapshots of Figure 2, corresponds to an intact stable double helix of DNA over 140 ps of MD simulation. The root-mean-square (rms) deviations of the dynamical structure from canonical forms, Figure 1c, show the calculated structure at the termination of the trajectory to be located ~2.3 Å rms from B80 and ~6.2 Å rms from A72, and thus clearly residing in the B-DNA family. The conformational parameters (Figures 4 and 5) are essentially stable or else show correlated transitions such as crankshaft motion in α and γ which conserve secondary structure in the helix. The observed conformational dynamics is consistent with the general ideas about backbone flexibility advanced some time ago by Olson,[63] although which transitions actually occur in the simulation is new information. In the helicoidal parameters, the behavior of XDP as a function of time indicates that the dynamical model is essentially a B form of DNA with a tendency toward an inclination in the base pairs approaching that of an A-form structure. A large propeller twist (~30–40°) in the base pairs is uniformly present. Base pair rise and twist are generally consistent with B-form DNA values. Values of ROL in the region of the axis deformations indicate an opening toward the minor groove, coupled with a slight tendency of the helix to underwind from the canonical value of 36 to ~30°.

The dynamics of the helical axis of the dodecamer is shown in Figure 11. The model shows a definite propensity for axis deformation in the vicinity of C3 and G10. The axis dynamics is also represented by the difference plot of path length minus end-to-end distance in Figure 12. This shows the axis deformations in the model to be oscillatory with an estimated frequency of ~10 cm^{-1}.

The behavior of the major and minor groove widths of the model is shown in Figures 13 and 14, showing the groove widths to be dynamically stable. The major groove is observed to be slightly but significantly reduced as compared with that of the canonical form except at one place (P4-P15), where the widths are similar. The minor groove shows a slight narrowing at the upper roll point even though the base pairs roll open at this point. Everywhere else, the minor groove is consistently wider than that of the canonical form.

The calculated dynamical structure resides at ~2.6 Å rms deviation from the native HD dodecamer crystal structure, slightly but significantly further than it is from B80. The CDW analysis of the crystallographic dodecamer has been discussed in some detail in a previous article.[9] The values of the conformational and helicoidal parameters for the HD dodecamer are given as dashed lines in Figures 4, 5, and 7–10. The (ϵ,δ) pair of torsions are in the B_{II} form at G10 and C23 in the crystal structure. The calculation shows no tendency to transit spontaneously from B_I to B_{II} values at these positions, but a stable B_{II} form occurs at C1 in the calculation and a $B_I \rightarrow (B_{II}) \rightarrow B_I$ transition is seen at A17. The crystal structure shows uniform behavior in (α,γ) of (g^-,g^+) whereas the dynamical structure shows considerable correlated conformational activity at these positions in 25% of the cases. The rms deviation of the 183 conformation angles of the dynamical structure is plotted as a function of time with respect to B80, A72, and the crystal structure of the native HD dodecamer in Figure 15a. The calculated results lie virtually equidistant from the crystal structure and from B80 and well differentiated from A72.

In the helicoidal parameters, the large negative propeller is a prominent feature of both the calculated and the crystallographic forms. The base pair inclination observed in calculated structure is not present in the crystal structure. There is however evidence from flow circular dichroism studies by Johnson and co-workers[69] that the DNA bases are tilted in solution. The rms deviation of the calculated helicoidal distances and angles from B80, A72, and the crystal structure is also shown in Figure 15. The dynamical structure is slightly closer to B80 than to HD based on helicoidal

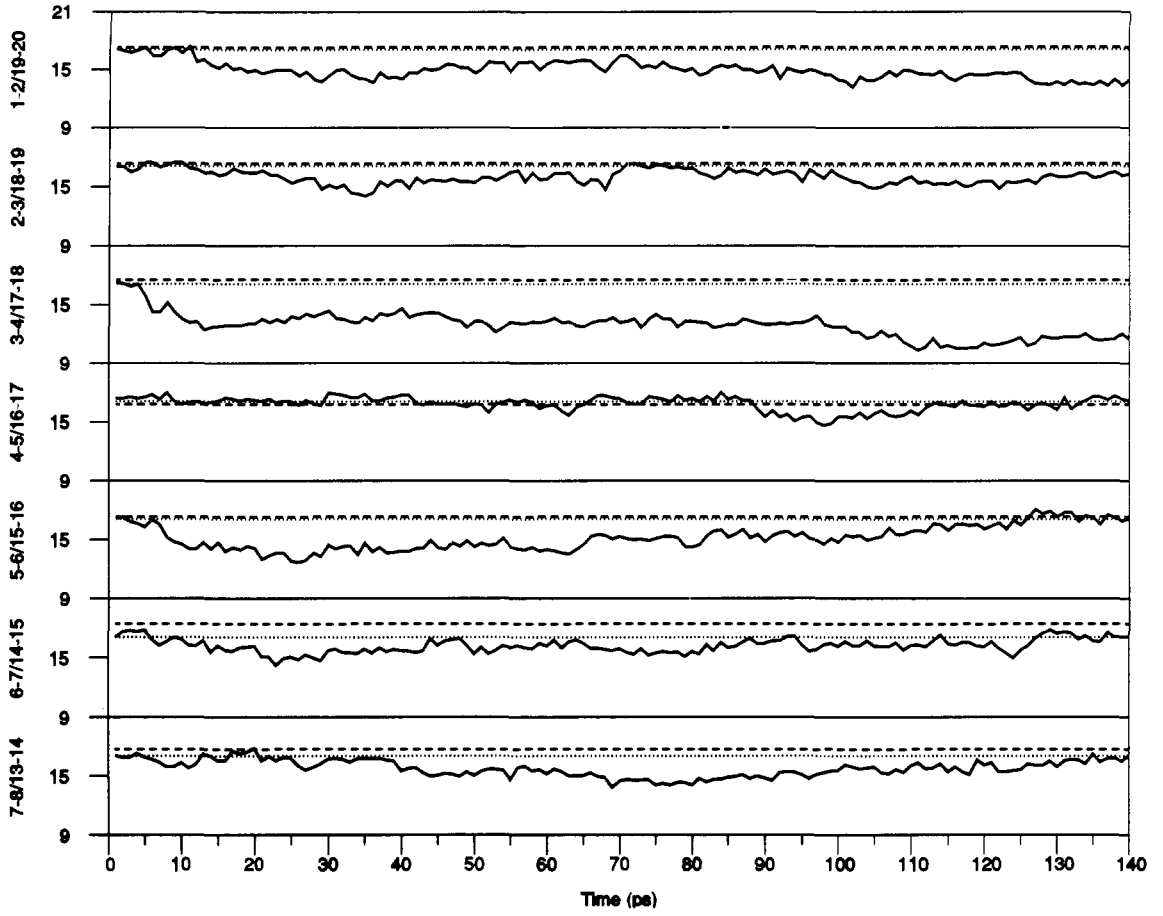

Figure 14. Calculated dynamical behavior of the minor groove inter-phosphate distances (Å) for the dodecamer at various points in the sequence as a function of time: (---) canonical B80 values, (···) native dodecamer.

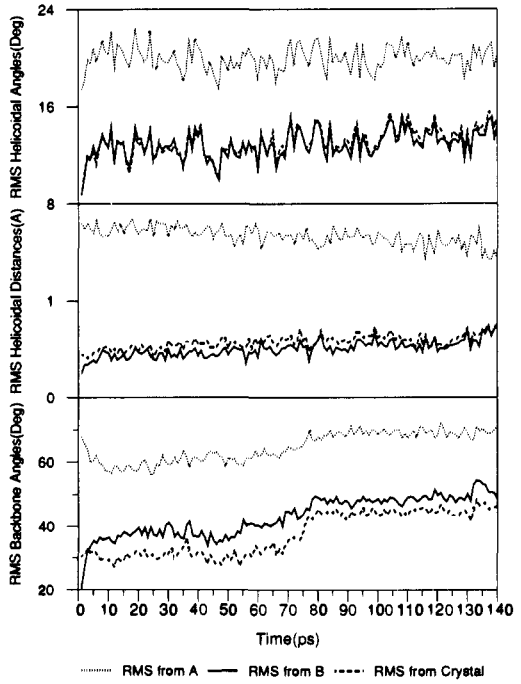

Figure 15. Calculated rms deviation of (a, top) conformational angles, (b, middle) helicoidal distances, and (c, bottom) helicoidal angles vs time for the 140-ps dynamical structure of the dodecamer.

distances, but significantly closer to the HD crystal structure in the helicoidal angles. The parameter PRP is no doubt the significant factor here.

The crystallographic values for the major and minor groove widths along the dodecamer helix are also indicated on Figures 13 and 14. The narrowing of the minor groove in the AT region of the crystal structure is not reproduced spontaneously in the MD over the time scale studied. The minor groove in the crystal dodecamer is expanded in the GC region, where helix–helix contacts occur. The narrowing in the AT region could be simply a mechanical response, and thus an indirect effect of crystal packing. The simulation as configured here would thus not be expected to reproduce this behavior. Exactly what are and are not packing effects in oligonucleotide crystals remains to be definitively resolved.[38]

The axis deformations observed in the crystal as the primary and secondary roll points are also quite spontaneous features of the dynamical structure, and there is close accord (Figure 11) between the calculated and crystallographic results. This lends strong independent support to the idea that the observed bending is structural feature intrinsic to the DNA dodecamer, and not simply induced by crystal packing or protein binding. The intrinsic propensity of the molecule to deform at these positions could easily lead to exaggerated deformations when packing effects or ligand binding are involved. The position of the axis deformation is primarily correlated with a slight but significant displacement in ROL (Figure 9), and thus what is seen in the simulation can be described as a "roll bend" with a slight contribution from TWS. This occurs at or near the roll points of the crystal structure. However, the roll opens the base pair step toward the minor groove in the calculation whereas the crystal structure shows ROL opening toward the major groove at the corresponding point, followed in the next step by a ROL opening toward the minor groove.

The calculated dynamical structure for the dodecamer in solution shows little accord with that proposed by Nerdal,[54] beyond of course the general loci of axis bending. Particularly there is no tendency for the DNA in the calculation to assume the highly underwound form indicated by the NMR data. A more detailed consideration of the solution structure of the dodecamer from both

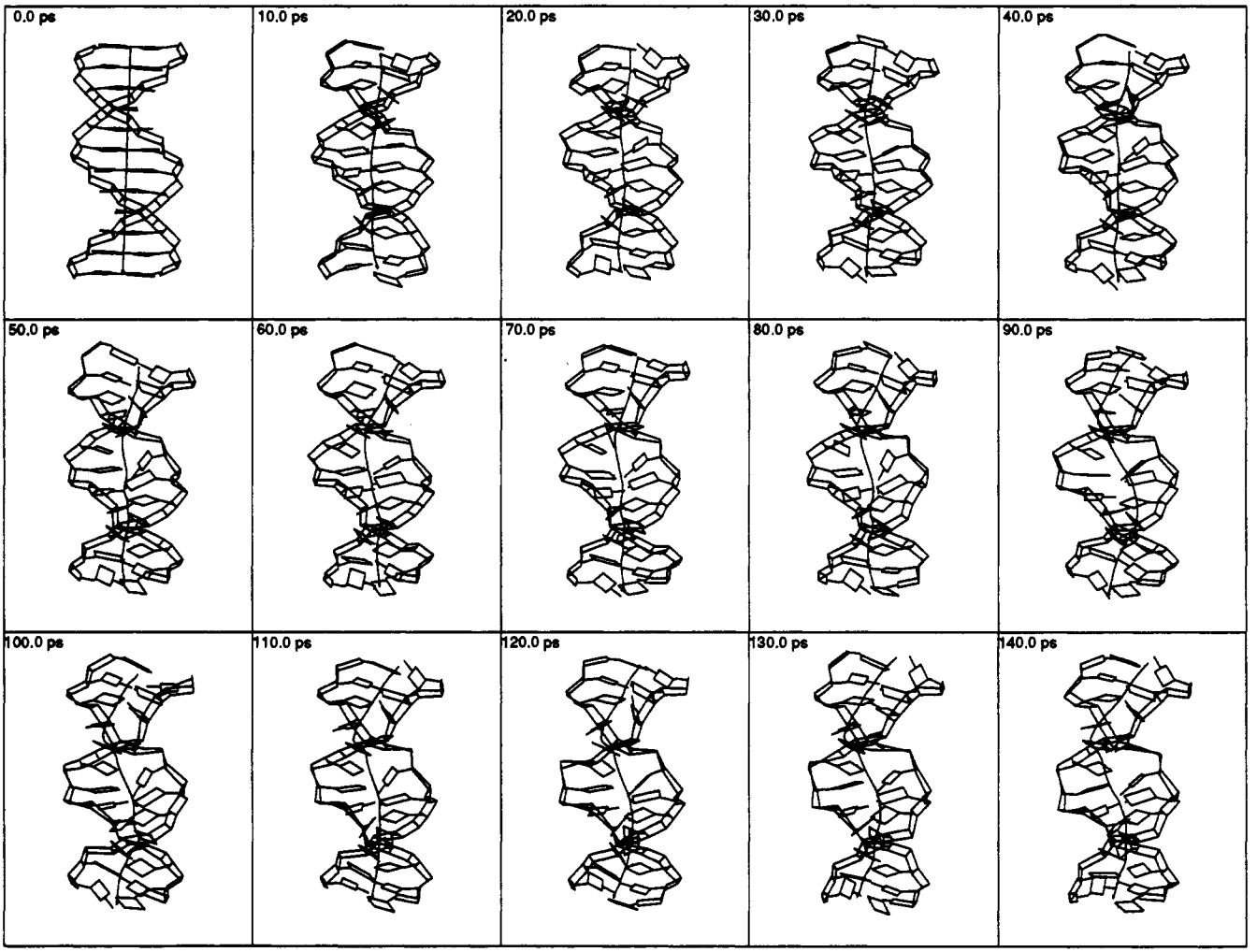

Figure 16. A sequence of snapshots from the MD trajectory calculated for the dodecamer in solution in the absence of the Watson–Crick base pairing constraint function.

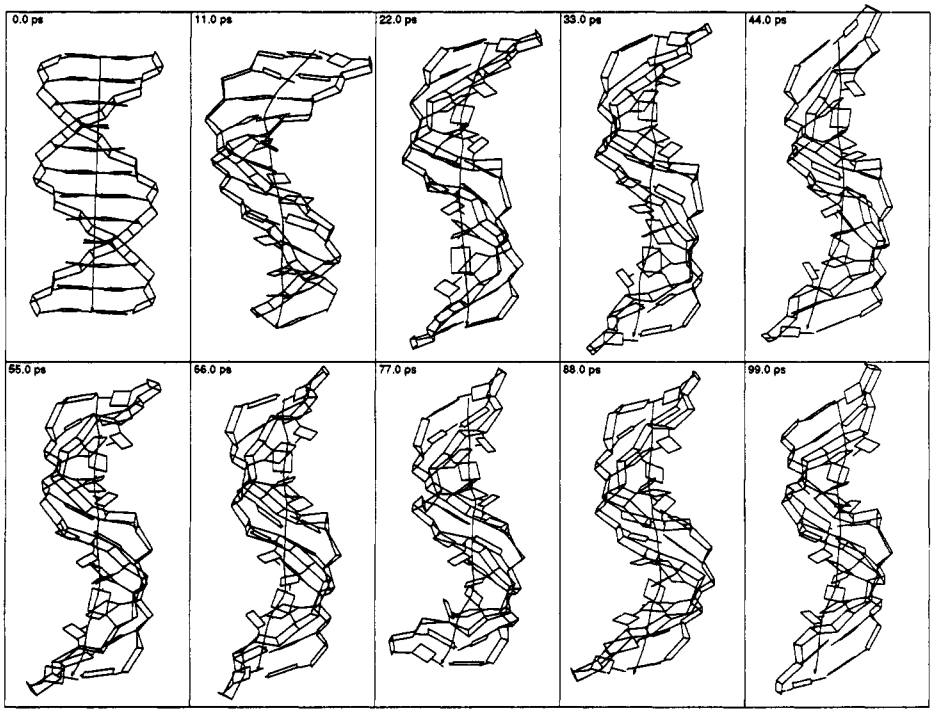

Figure 17. A sequence of snapshots from the MD trajectory calculated for an in vacuo simulation of d(CGCGAATTCGCG), including the Watson–Crick base pairing constraint function.[59]

NMR and molecular dynamics will be forthcoming.

The hydration[70-72] and counterion atmosphere[73,74] of the dodecamer have been the subjects of ongoing studies in this group based on Monte Carlo simulation. The detailed analysis of the dynamical hydration and counterion structure will be the subject of a forthcoming paper. Briefly, the calculated hydration density of the minor groove of the dodecamer reveals an ordered water structure in the minor groove to be well-developed in the calculation. The counterion density is seen to imply a structure where the counterions are arrayed in an irregular manner along the DNA backbone. No indication of a tendency of the counterions to penetrate the grooves of DNA was observed in the calculation. The counterion density is seen to imply a structure where the counterions are arrayed in an irregular manner along the DNA backbone. No indication of a tendency of the counterions to penetrate the grooves of DNA was observed in the calculation.

Finally, we present two simulations which, in comparison with the study described above, convey an idea of the sensitivity of the results to certain aspects of the force field and the effect of solvent. The addition of a restraint function for Watson–Crick hydrogen bonds was introduced in the simulation to assure our model is consistent with the clear indication from NMR that base pairing is maintained in solution. Hydrogen exchange in base pairs occurs only in the range of once per millisecond,[48] far beyond the picosecond time scale. We have explored what happens when this restraint is removed and there is only the electrostatic charge on the atoms to establish hydrogen bonding. The results of a 140-ps simulation carried out with no WC restraint function are shown in the series of snapshots given in Figure 16. The simulation retains B-form helical characteristics, but detailed analysis shows higher amplitude buckling of the base pairs. An exaggerated deformation (kink) of the helix is observed at C3pG4 due to a combination of displacement base pair OPN, SHF, and SLD. The WC base pairing is disrupted and significant expansion of the minor groove is observed when and where the kink occurs. These effects persist for the remainder of the trajectory. The coupling of axis bending and base pair opening has been noted elsewhere.[75] Due to the obvious deviation from available experimental data, we do not presume this to be an accurate dynamical model of DNA. In the previous WC simulation, we noted an increase in the restraint energy during the bending process, further evidence of a coupling between bending and base pair opening.

An in vacuo simulation of 100 ps analogous to the in aquo case described above has also been carried out.[59] This simulation is based on the GROMOS force field with WC restraints. A reduced charge of −0.25 was assigned to each phosphate, and 22 Na^+ sized solvatons of charge +0.25 were introduced to establish electroneutrality. The results are shown in Figure 17. Here one obtains a well-defined B-form helix, but ~5 Å from both the canonical B80 structure and the HD crystal structure of the dodecamer. The singular feature of this structure is a pronounced narrowing, almost a collapse, of the minor groove. The presence of water in the simulation thus appears to be important in supporting a proper groove structure in the model DNA. Other features of interest are a uniform negative INC, higher amplitude BKL and PRP, and considerable sequence dependence in ROL and TWS. Charges of −1 on the phosphate and +1 on the counterions led to an unstable helix in a dielectric of $\epsilon = 1$, consistent with the results found earlier by Levitt.[2]

A complete set of full size Dials and Windows for all three simulations reported here are available on request from the authors.

VI. Summary

The dynamical model of d(CGCGAATTCGCG) obtained in this study resides clearly in the B family of the DNA structure, some 2.0 rms deviation from the corresponding canonical B form. The analysis of the simulation reveals good accord with a number of features seen in the X-ray crystal structure of the dodecamer, including local axis deformation near the GC/AT interfaces in the sequence and large propeller twist in the base pairs. The DNA base pairs show a consistent inclination in the simulation, in accord with the result obtained from flow dichroism studies of DNA in solution. Some features of the crystal structure, such as narrowing of the minor groove in the AT region, are not seen over the time course of the simulation. It is not completely clear at this point in time which of these features are due to crystal packing and which are intrinsic to the DNA, and of course only the latter are expected to appear in the simulation described herein. The dynamical structure shows little quantitative agreement with the NMR structure of the dodecamer in solution recently proposed by Reid and co-workers. Subsequent simulations show that without the Watson–Crick restraint function, more pronounced axis deformations are observed and explicit inclusion of the water molecules in the simulation is necessary to properly support the major and minor groove structure of the DNA helix.

Overall, the model produced here exhibits quite reasonable behavior in light of what is known experimentally about DNA solution structure at this point in time, and is clearly worth further consideration. We are currently extending these simulations to other sequences for which experimental data are available and attempting a systematic study of DNA fine structure and bending on this basis. A companion paper[76] presents the NOE buildup curves calculated on the basis of the MD trajectories described herein.

Acknowledgment. This research was supported by grants to D.L.B. from the National Institutes of Health (GM-37909) and the Bristol-Myers Corporation via participation in a State of Connecticut Cooperative High Technology Research and Development Grant. Computer time on the CRAY YMP was provided by the Pittsburgh Supercomputer Center. The provision of results for the in vacuo GROMOS simulation by J. Srinivasan, the assistance of J. Withka on preparing some of the figures, and discussions on this work with Profs. H. M. Berman, W. Olson, and R. E. Dickerson are gratefully acknowledged.

Registry No. d(CGCGAATTCGCG), 77889-82-8.

(70) Subramanian, P. S.; Ravishanker, G.; Beveridge, D. L. *Proc. Natl. Acad. Sci. U.S.A.* **1988**, *85*, 1836.
(71) Subramanian, P. S.; Beveridge, D. L. *J. Biomol. Struct. Dyn.* **1989**, *6*, 1093.
(72) Subramanian, P. S.; Swaminathan, S.; Beveridge, D. L. *J. Biomol. Struct. Dyn.* **1990**, *7*, 1161.
(73) Jayaram, B.; Swaminathan, S.; Beveridge, D. L.; Sharp, K.; Honig, B. *J. Phys. Chem.* **1990**, *23*, 3156.
(74) Jayaram, B.; Beveridge, D. L. *J. Phys. Chem.* In press.
(75) Ramstein, J.; Lavery, R. *Proc. Natl. Acad. Sci. U.S.A.* **1988**, *85*, 7231.
(76) Withka, J. M. *NMR and Molecular Dynamics Studies of Intact and Damaged DNA Sequences*. Ph.D. Thesis, Wesleyan University, 1991.
(77) Davies, D. B.; Altona, C.; Arnott, S.; Danyluk, S. S.; Hruska, F. E.; Klug, A.; Ludeman, H. D.; Pullman, B.; Ramachandran, G. N.; Rich, A.; Saenger, W.; Sarma, R. H.; Sudaralingam, M. *Eur. J. Biochem.* **1983**, *131*, 9.